

FRACTURE TOUGHNESS AND FRACTURE PROCESSES IN DUCTILE METALLIC FOAMS

C. Motz and R. Pippan

Erich Schmid Institute of Material Science,
Austrian Academy of Sciences, A-8700 Leoben, Austria

ABSTRACT

For structural applications of aluminium foams, besides tensile and compressive behaviour, fatigue and energy absorbing the fracture mechanic behaviour is important. Fracture mechanic tests were performed on compact tension (CT) specimens of sizes from $W=50$ mm to $W=300$ mm made of ALPORAS® foams with different densities. In addition to standard tests, in-situ fracture experiments in a scanning electron microscope were performed. Besides the load and the load line displacement also crack extension via a potential drop technique, crack tip opening displacement and local deformations were measured. The deformation is strongly localized on different length scales. In front of the notch root a fracture process zone with concentrated deformation develops. The crack propagates through the foam building many secondary cracks and crack bridges. The determination of fracture toughness values in terms of stress intensity factor K , J -integral and crack tip opening displacement is discussed. The comparison of the K vs. Δa (crack extension), J vs. Δa and COD vs. Δa with the actual fracture processes at the crack tip and load displacement response reveals that COD_5 gives the most reliable values to characterize the fracture toughness. The critical values for COD_5 range from 0.35 mm to 1.0 mm depending on the relative density of the foam.

KEYWORDS

metallic foams, cellular solids, fracture toughness, fracture processes, local deformation.

INTRODUCTION

In the last few years metallic foams, e.g. made of aluminium or magnesium alloys, have become commercially available due to improvements in the manufacturing processes. This new class of materials exhibits partly unusual mechanical properties compared to common metals. For successful design of load bearing structural elements, besides the well-investigated compression and energy absorbing behaviour [1-4], also the fracture behaviour and fracture toughness values are needed. Until now only a limited number of publications [5-7] addressing this topic are available. The aim of this investigation is to provide a closer look at fracture processes and the determination of fracture toughness values for these foams. Thus, standard fracture mechanic tests and additionally in-situ fracture tests in the scanning electron microscope were performed to determine fracture processes and fracture toughness values. For the tests, an ALPORAS® aluminium foam, which is commercially available, with different densities was used. Standard fracture mechanic parameters, like stress intensity factor K , J -integral and crack opening displacement COD , were

determined. All investigations were accompanied with local surface strain measurements, which show the development of the fracture process zone during crack initiation and crack propagation.

EXPERIMENTAL SETUP

Specimen preparation

All investigations were carried out on ALPORAS® aluminium foams with two densities, 0.25 g/cm³ and 0.40 g/cm³. Chemical composition, production route and material properties of these foams are described in [8]. Standard compact tension (CT) specimens with a size range of W=50 mm to W=300 mm and a thickness of B=30 mm were used. The specimens were machined with a diamond wire saw to avoid damage of the foam. All specimens had an open surface, whereby the average cell size of the foam was about 3.5 mm. For the pre-crack a diamond wire saw cut with a notch tip radius of about 150 µm was used, which gave undistinguishable experimental results compared to specimens pre-cracked in fatigue (see also [9]).

Standard fracture mechanic tests

Standard fracture mechanic tests were carried out on a displacement controlled universal mechanic testing machine at room temperature and at a cross-head speed of 0.2 mm/min for specimen sizes W≤100 mm and 0.5 mm/min for W>100 mm. The load and the load line displacement were measured with a standard load cell and a clip gauge, respectively. Additionally, the crack or notch opening displacement (COD) was determined with a videoextensometer 5 mm behind the initial crack tip. The crack extension was monitored by a potential drop technique and was verified by optical observations. Images from the foam surface were taken at different load line displacements with a CCD-camera at a resolution of 1528x1146 pixels and were used for local surface deformation measurements and for documentation of the crack extension, subsequently. The procedure for local deformation measurements is described in detail in [10].

In-situ experiments

In order to investigate crack initiation, crack propagation and local deformations during crack growth, in-situ fracture tests in the scanning electron microscope (SEM) were performed. Due to the restricted space inside the SEM the specimen size is limited to W=50 mm and B=25 mm. A small in-situ loading device, with a displacement rate of 0.15 mm/min, was used to fracture the CT-specimens. In order to assign the different stages of the fracture process to the load versus load line displacement curve, the load and the displacement were measured too. Images from the foam surface, containing 1 to 6 cells, with a resolution up to 4000x3200 pixels were taken at different load line displacements. Subsequently, these images were analysed to measure crack extension, local deformations and to identify the fracture processes.

RESULTS AND DISCUSSION

Standard fracture mechanic tests

Due to the somewhat unusual mechanical behaviour of ductile metallic foams, e.g. a marked stress plateau in compression, a deformation dependence of the Young's modulus or strain localisation during deformation, also in the fracture mechanics tests some atypical effects can be expected. Fig. 1 shows a typical load F and crack extension Δa versus load line displacement v_{LLD} curve and a corresponding surface deformation map for a foam with a density of 0.40 g/cm³. It is evident from the load curve that these foams reveal only a very small linear elastic stage, followed by an extended plastic regime. The plastic deformation is strongly localised in a fracture process zone (FPZ), which can be seen in the surface strain maps and can result in micro cracking of some high strained cell walls. In the region of the peak load a main crack starts from the notch root and propagates in a relatively large FPZ through the specimen, whereby the load decreases. This is usually accompanied with a characteristic kink in the crack extension curve, followed by a regime of larger crack growth rate. Both, the load and the crack extension curve, show in the region of stable crack growth a certain waviness, which is related to the inhomogeneous structure of the foam and results in a variation in the local crack growth resistance.

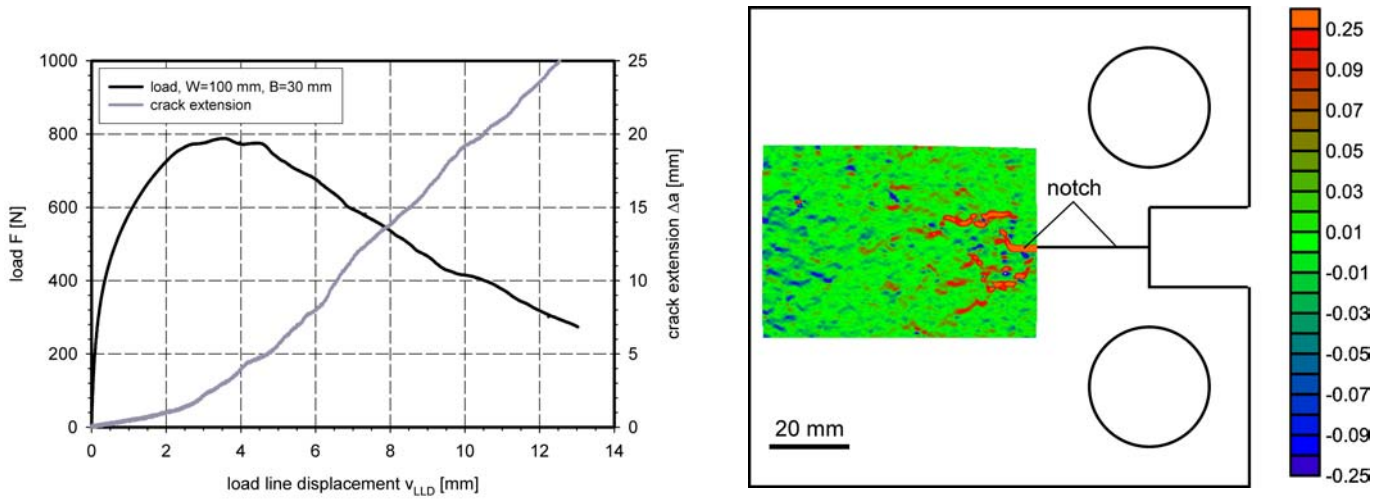


Figure 1 Load and crack extension versus load line displacement curve (left image) and corresponding surface strain map at a crack extension of 5 mm (right image, $\epsilon = \times 100\%$) for an ALPORAS® aluminium foam CT-specimen with a density of 0.40 g/cm^3 , $W=100 \text{ mm}$ and $B=30 \text{ mm}$.

Because of the wide plastic regime in the load versus load line displacement curve no valid fracture toughness values in terms of the critical stress intensity factor K_{IC} according to ASTM E399 could be obtained with the specimen sizes used in this investigation. The calculated K_Q values are relatively low and vary between 0.35 to $1.0 \text{ MPa}\cdot\text{m}^{1/2}$ depending on the density of the foam. Fig. 2 shows K versus crack extension Δa curves for two foams with different densities. Both foams reveal an increase of the fracture toughness with crack propagation up to a crack extension of about 5 mm (it looks like a R-curve behaviour). This toughness enhancement with increasing Δa is caused by plasticity, but also toughening mechanisms like crack bridging [6] and the formation of a FPZ containing localised yielding and micro cracking may contribute. In the region of larger crack extensions a decrease of K can be observed, which is dramatically in the case of the lower density foam. The “softening mechanisms” that are causing this drop in K (and also in the plastic limit load ratio F/F_Y) are not clear until now.

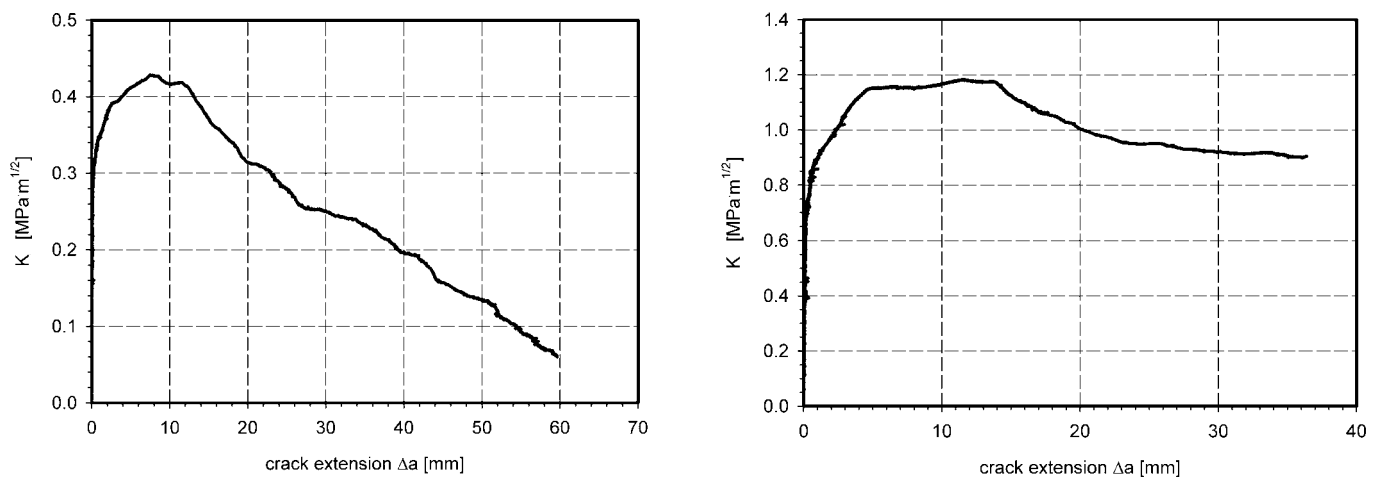


Figure 2 Stress intensity factor K versus crack extension Δa curve for two foams with a density of 0.25 g/cm^3 (left image) and 0.40 g/cm^3 (right image). CT-specimens with $W=290 \text{ mm}$ and $B=30 \text{ mm}$ were used.

Fig. 3 shows the load - plastic limit load ratio versus load line displacement plots for the same two foams as depicted in Fig. 2. Also in the load - plastic limit load ratio F/F_Y (load divided by the corresponding plastic limit load) curves a significant drop in the region of larger crack extensions (or larger load line displacements) can be observed. Especially the lower density foam (0.25 g/cm^3) reveals a dramatically drop in the plastic limit load ratio. It seems that both foams do not reach the stage of full plastification ($F/F_Y=1$). But due to the very small linear elastic regime of these foams it is difficult to measure the yield stress σ_y . So

the absolute values of the F/F_Y ratios depend on the chosen yield stress and may differ slightly, if $\sigma_{0.1}$, $\sigma_{0.2}$ or $\sigma_{0.5}$ are used for the yield strength.

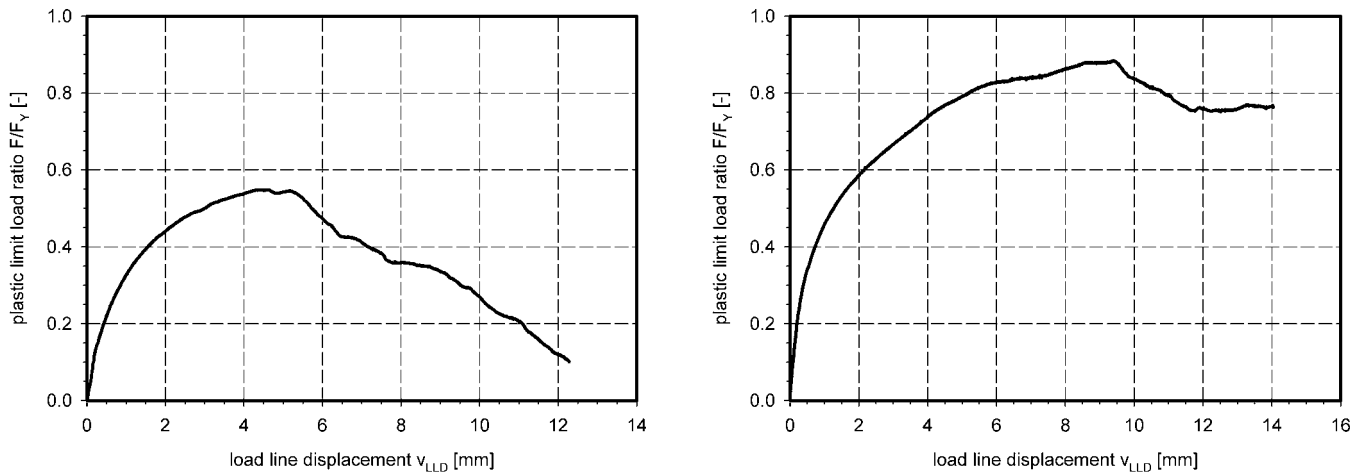


Figure 3 Plastic limit load ratio F/F_Y versus load line displacement curves for the two foams, which are depicted in Fig. 2. Left image shows the foam with the density of 0.25 g/cm^3 and the right image the foam with 0.40 g/cm^3 .

Since valid fracture toughness values based on K_{IC} could not be obtained in these tests, single specimen J-integral determinations according to ASTM standard E813 and E1152 were performed. Fig. 4 shows J-integral versus crack extension plots for different specimen sizes and different foam densities. Although in all J-integral tests the specimen size criterion was fulfilled, a certain size dependence of the initial J-value $J_{0.2}$ and the J-curve can be observed. Furthermore, the initial part of the J-integral curves shows an atypical shape and a large scatter, which makes the determination of initial J-values, like J_i or $J_{0.2}$, according to the standards difficult or impossible. A typical plateau in the J-integral curves that is associated with a steady state J-value J_{SS} , as reported in [6], cannot be observed in all samples. For the foams with lower densities a decrease in the J-integral curve at large crack extensions is evident. This is in agreement with the previous observations in the K vs. Δa and F/F_Y vs. v_{LLD} curves. In general, the application of ASTM standards (E813, E1152), which are designed for solid metals, to metallic foams is problematic. Due to their special mechanical behaviour, metallic foams exhibit a different response in the fracture mechanic tests as assumed in common standards.

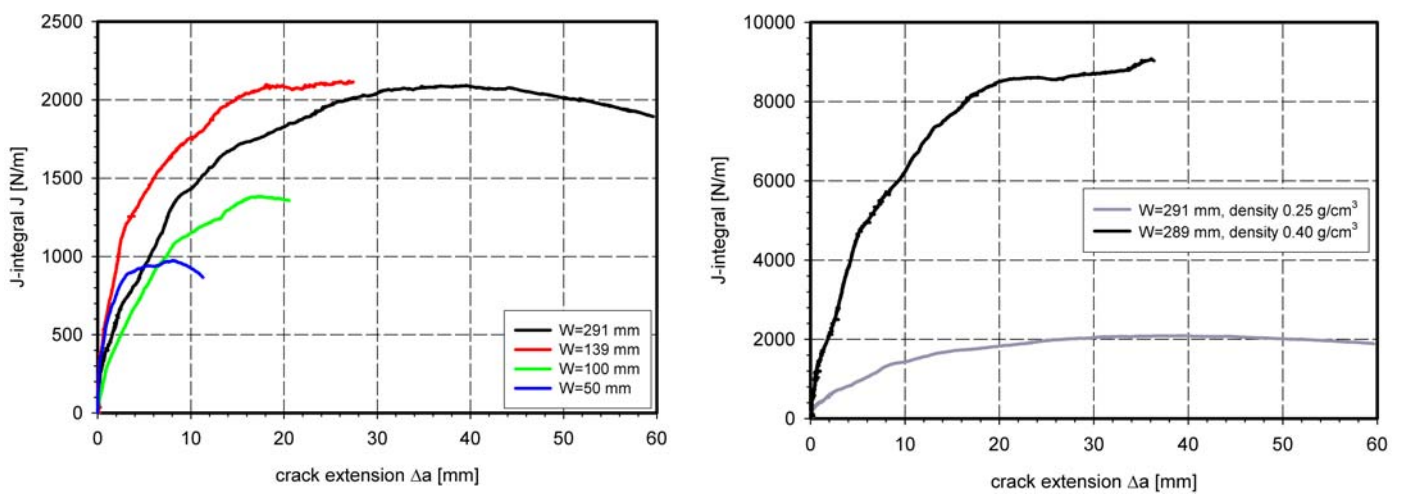


Figure 4 J-integral versus crack extension plots for different specimen sizes and at a constant density of 0.25 g/cm^3 (left image) and for different densities at constant specimen size (right image).

The described methods calculate from the global mechanical response the fracture toughness values (stress intensity factor K , J-integral). A more direct method is provided by the crack opening displacement (COD) concept. In this investigation the COD_5 value is used, which is measured 5 mm behind the initial crack tip or

notch root [11]. Fig. 5 shows COD₅ and CTOD (crack “tip” opening displacement, which is determined 5 mm behind the actual crack tip; in our case this corresponds to 1.5 times the mean cell diameter) versus crack extension curves for two foams with different densities. It was found that the COD₅ curves show a characteristic kink at low crack extensions (about ½ of the mean cell diameter), which can be associated with an “initial” fracture toughness value. The CTOD curves that deliver an actual fracture toughness value did not show a decrease at larger crack extensions, which is in contrast to the K vs. Δa and J vs. Δa curves. It seems that the possible softening mechanisms do not influence the resistance against crack propagation in terms of CTOD or crack tip opening angle, but have an impact on the general mechanical behaviour of the CT-specimens. Further detailed investigations are needed to identify the softening mechanisms and to find an appropriate method for the determination of fracture toughness values in terms of J.

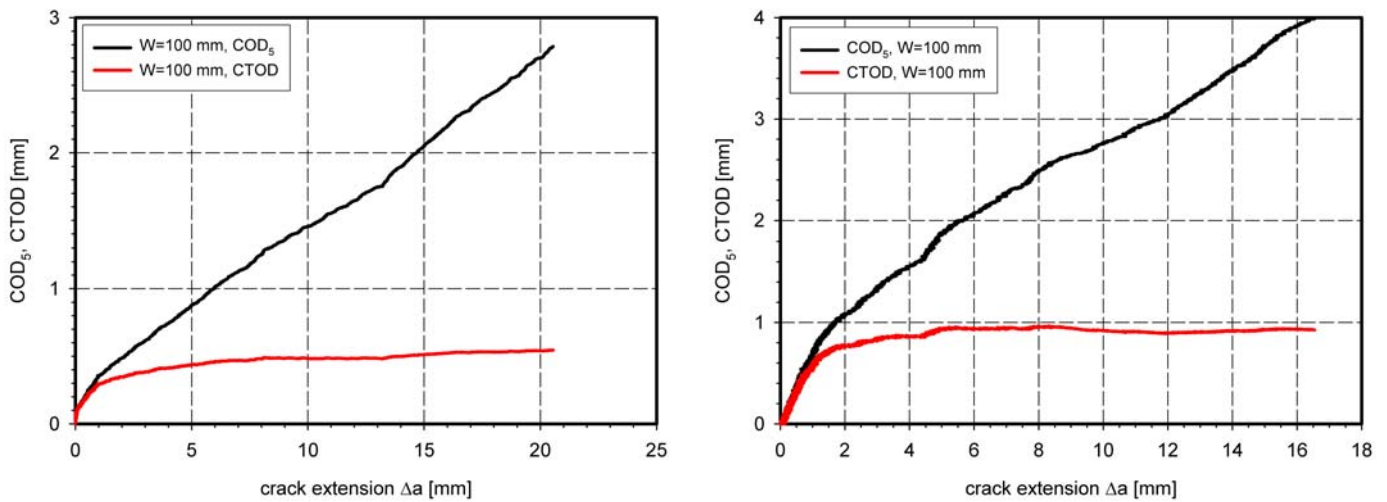


Figure 5 COD₅ and CTOD versus crack extension curves for two foams with different densities, 0.25 g/cm³ (left image) and 0.40 g/cm³ (right image).

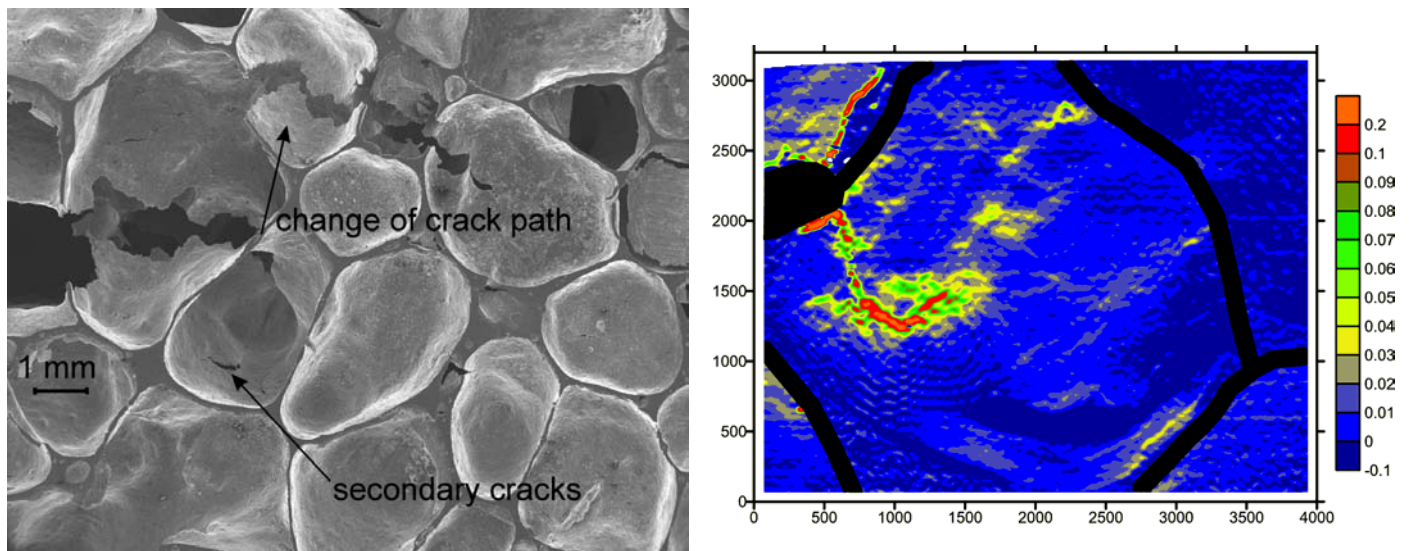


Figure 6 SEM micrograph from the region in front of the notch root of an in-situ cracked CT-specimen after a crack extension of about 6 mm (left image) and local in-cell-wall strain map from the first cell in front of the notch root at crack initiation, showing the plastic zone (right image, 4000 pixels are equivalent 3.3 mm). Strains are given in loading direction, $\epsilon = \times 100\%$, and the black lines mark the boundaries of the cells.

In-situ fracture tests

With a small loading device in-situ fracture tests in the scanning electron microscope (SEM) were performed to investigate the fracture processes. Loading of the specimen results in a very early, inhomogeneous plastic deformation of the foam. The strains are localised on different length scales. On the lower level, the cell walls, only some small regions in the walls are deformed, whereby the rest remains nearly undeformed. An

example is depicted in Fig. 6. On the higher length scale, the cell structure, only few weaker cells show larger deformations (see Fig. 1). With increasing load a fracture process zone develops in front of the notch root, which contains localised plastic yielding and micro cracking. At about 80% of the peak load a main crack starts from the notch root to propagate through the foam structure. This is accompanied by building of crack bridges up to 1 - 3 cell sizes behind the crack tip and by micro cracking of cell walls in the FPZ (see Fig. 6). The crack follows the path of lowest fracture resistance, which is in general the path with the thinnest cell walls.

CONCLUSION

Standard fracture mechanic tests based on the stress intensity factor, the J-integral and the COD concept were performed on ALPORAS® aluminium foams with different densities. Additionally, in-situ fracture tests in the SEM and local surface deformation measurements were carried out. The surface strain measurements reveal a very localised deformation of the foam on different length scales. During the crack growth a large fracture process zone develops, which contains localised plastic yielding and micro cracking of several cell walls. Due to the very small linear elastic part in the load versus load line displacement curve no valid K_{IC} values according to ASTM E399 could be obtained. Although all performed J-integral tests were valid, the standard determination of fracture toughness values in terms of an initial J-value is not useful. The ASTM standards are optimised for solid metals and their application to ductile metallic foams is usually not possible and they should be adapted to the special properties of the foams. It was found that measurements of crack opening displacement in terms of COD_5 gives a better approach to useful fracture toughness values.

ACKNOWLEDGEMENT

The financial support by the Austrian Fonds zur Förderung der wissenschaftlichen Forschung and of the Österreichischen Nationalbankfonds (Project P13231PHY/FWF535) is gratefully acknowledged.

REFERENCES

1. H. Bart-Smith, A.-F. Bastawros, D. R. Mumm, A. G. Evans, D. J. Sypeck, H. N. G. Wadley, (1998) *Acta Mater.* 46, 10, 3583-3592
2. H. Fusheng, Z. Zhengang, G. Junchang, (1998) *Metall. and Mat. Trans.* 29A, 2497-2502
3. R. Gradinger, F. G. Rammerstorfer, (1999) *Acta Mater.* 47, 1, 143-148
4. E. Andrews, W. Sanders, L.J. Gibson, (1999) *Mat. Science and Eng.* A270, 113-124
5. Y. Sugimura, J. Meyer, M.Y. He, H. Bart-Smith, J. Grenstedt, A.G. Evans, (1997) *Acta Mater.* 45, 12, 5245-5259
6. O.B. Olurin, N.A. Fleck, M.F. Ashby, (2000) *Mat. Science and Eng.* A291, 136-146
7. C. Motz, R. Pippan, Proc. ECF13, M. Fuentes, M. Elices, A. Martin-Meizoso & J.M. Martinez-Esnaola, Eds., Elsevier Sciences (2000), 160c1.pdf (CDROM), 1-8
8. T. Miyoshi, M. Itoh, S. Akiyama, A. Kitahara, (2000) *Adv. Eng. Materials* 2, No. 4, 179-183
9. K.Y.G. McCullough, N.A. Fleck, M.F. Ashby, (1999) *Acta Mater.* 47, 2331-2343
10. A. Tatschl (2000), *Neue experimentelle Methoden zur Charakterisierung von Verformungsvorgängen*, Ph.D. thesis, University of Leoben, Austria
11. K.H. Schwalbe, A. Cornec, *Fatigue of Eng. Mat.* (1991), 14, 405-412